

Radiocarbon

<http://journals.cambridge.org/RDC>

Additional services for **Radiocarbon**:

Email alerts: [Click here](#)

Subscriptions: [Click here](#)

Commercial reprints: [Click here](#)

Terms of use : [Click here](#)

Historical Reconstruction of Submarine Earthquakes Using ^{210}Pb , ^{137}Cs , and ^{241}Am Turbidite Chronology and Radiocarbon Reservoir Age Estimation off East Taiwan

L Dezileau, R Lehu, S Lallemand, S-K Hsu, N Babonneau, G Ratzov, A T Lin and S Dominguez

Radiocarbon / *FirstView* Article / January 2016, pp 1 - 12

DOI: 10.1017/RDC.2015.3, Published online: 21 January 2016

Link to this article: http://journals.cambridge.org/abstract_S003382221500003X

How to cite this article:

L Dezileau, R Lehu, S Lallemand, S-K Hsu, N Babonneau, G Ratzov, A T Lin and S Dominguez Historical Reconstruction of Submarine Earthquakes Using ^{210}Pb , ^{137}Cs , and ^{241}Am Turbidite Chronology and Radiocarbon Reservoir Age Estimation off East Taiwan. *Radiocarbon*, Available on CJO 2016 doi:10.1017/RDC.2015.3

Request Permissions : [Click here](#)

HISTORICAL RECONSTRUCTION OF SUBMARINE EARTHQUAKES USING ^{210}Pb , ^{137}Cs , AND ^{241}Am TURBIDITE CHRONOLOGY AND RADIOCARBON RESERVOIR AGE ESTIMATION OFF EAST TAIWAN

L Dezileau^{1,2*} • R Lehu^{1,3} • S Lallemand^{1,2} • S-K Hsu^{2,3} • N Babonneau^{2,4} • G Ratzov⁵ • A T Lin^{2,3} • S Dominguez^{1,2}

¹Université de Montpellier, Géosciences Montpellier, CNRS, France.

²LIA ADEPT, NSC-CNRS, France-Taiwan.

³Department of Earth Sciences, National Central University, Zhongli, Taiwan (R.O.C).

⁴Domaines Oceaniques, IUEM, Brest, France.

⁵Université Nice Sophia Antipolis, CNRS, IRD, Observatoire de la Côte d'Azur, Géoazur UMR 7329, 250 rue Albert Einstein, Sophia Antipolis 06560 Valbonne, France.

ABSTRACT. Taiwan is a young and seismically active mountain belt, where a series of strong earthquakes ($M > 7$) have occurred over the past hundred years. Identifying historical earthquakes around Taiwan is a key to better constrain the geodynamic of this active region. Sedimentological and geochemical analyses of surface sediments from one station offshore east Taiwan revealed the presence of coarse-grained layers interpreted as turbidites. The age of these layers have been determined by ^{210}Pb , ^{137}Cs , and ^{241}Am chronology. Dating of the three most recent turbidites provides ages of AD 2001 \pm 3, AD 1950 \pm 5, and AD 1928 \pm 10. The results show striking temporal correspondence of turbidite layers to large ($M \geq 6.8$) earthquakes recorded in the region since the 20th century. The chronologies of sediment layers lead us to believe that turbidites resulted from the 2003 Taitung earthquake (M 6.8), the 1951 Chengkong earthquake (M 7.1), and the 1935 Lutaio earthquake (M 7.0), respectively. Such a good correlation between turbidites and high-magnitude ($M \geq 6.8$) historical and instrumental seismic events suggests that turbidite paleoseismology constitutes a valuable tool for earthquake assessment in the eastern Taiwan margin. Moreover, the modern reservoir radiocarbon age and the regional marine reservoir correction (ΔR) of the Kuroshio Current off Taiwan were estimated by comparing accelerator mass spectrometry (AMS) ^{14}C ages with ages derived from corrected ^{210}Pb profiles and historical accounts of identifiable seismic events. Such a determination is important to calibrate the ^{14}C ages of marine materials for accurate comparison of marine and continental geological records. Our calculated mean ΔR value of 232 ± 54 ^{14}C yr ($n = 2$) is higher than its modern value of 86 ± 40 ^{14}C yr. This high value can be explained by the presence of local upwelling cells and turbulence in the Kuroshio Current, north of Green Island. These upwelling cells bring ^{14}C -depleted water to the surface, resulting in an increase of the modern ΔR value in this portion of the Kuroshio Current.

KEYWORDS: Radiocarbon dating, reservoir age, paleoseismology, Taiwan, ^{137}Cs , ^{210}Pb , marine sediment, Holocene.

INTRODUCTION

The Taiwan orogen is a young and active mountain belt resulting from the rapid collision of the Luzon arc, carried by the Philippine Sea Plate, and the Chinese continental margin (Figure 1) (Biq 1972; Suppe 1984). In this region, plate convergence is extremely high, about 80 mm/yr (Seno et al. 1993). The seismicity rate is significant with more than 20 earthquakes $M > 7$ recorded for the last 100 yr, the largest of which was recorded in 1920, with a revisited magnitude of M 7.7 (Theunissen et al. 2010). Submarine landslides, and the resulting mass transport deposits or turbidite deposits, have been recognized in the Taiwan margin area in seismic and coring data (Lehu et al. 2015). Interpretation of sedimentary deposits on the eastern Taiwan submarine slope suggests a direct link between submarine gravity processes (submarine landslides and turbidity currents) and the occurrence of large earthquakes. In order to investigate the modern sedimentation (< 150 yr) associated with recent seismic events in the eastern Taiwan margin, a sediment core was collected by a box corer for radiometric (^{14}C , ^{210}Pb , ^{137}Cs , and ^{241}Am) and sedimentological analyses.

^{210}Pb ($T_{1/2} = 22.3$ yr) is a widely used radiotracer in the study of sedimentary environments on a temporal scale of 100–150 yr (e.g. Nittrouer et al. 1970; Robbins and Edgington 1975). This naturally occurring radionuclide forms in sediments by the decay of ^{222}Rn ($T_{1/2} = 3.8$ days) in the atmosphere and the water column (^{210}Pb excess) and *in situ* decay of

*Corresponding author. Present address: UMR5243 CC60 UM/CNRS, Place E. Bataillon 34095 Montpellier cedex 5, France. Email: laurent.dezileau@gm.univ-montp2.fr.

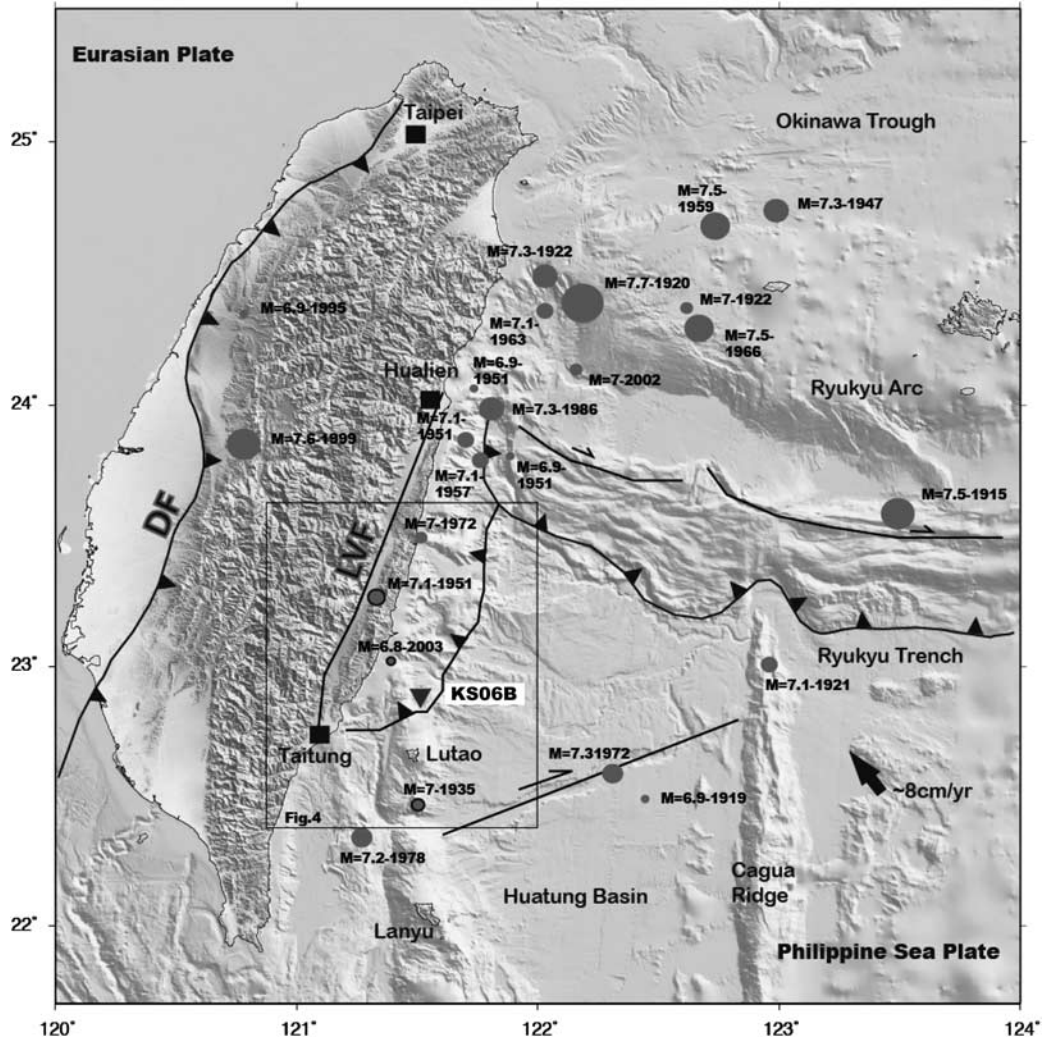


Figure 1 Map of Taiwan showing geodynamical setting and strong magnitude earthquakes ($M > 6.8$) over the last 100 yr. Two major on-land faults are represented: DF = Deformation Front; LVF = Longitudinal Valley Fault.

^{226}Ra ($T_{1/2} = 1600$ yr). Age models based on ^{210}Pb activity profiles in sediment cores can be confirmed by independent time-stratigraphic markers, such as artificial radionuclides (e.g. ^{137}Cs , ^{241}Am), which allow us to discriminate the influence of postdepositional processes such as mixing. An increase in the amount of ^{137}Cs in sediments corresponds to the beginning of atmospheric nuclear tests in the 1950s, and the highest concentrations correspond to the maximum atmospheric value reached in 1963.

An undisturbed sediment profile is characterized by an exponential decrease in ^{210}Pb activity with depth. However, the presence of rapid/instantaneous sedimentation deposits in slow sedimentation deposits induces irregularities in ^{210}Pb profiles. As this kind of deposit is of potential interest in paleoseismic studies, where turbidity flows can transport sediment from the margin slope, solving the problem of dating sediment records with nonlinear ^{210}Pb profiles is of wide interest (Arnaud et al. 2002; Huh et al. 2004, 2006; Garcia-Orellana et al. 2006).

The first aims of this paper are to date surface sediments from one station offshore east Taiwan, which revealed the presence of coarse-grained layers corresponding to turbidites by using the ^{210}Pb constant flux, constant sedimentation (CFCS) model constrained by ^{137}Cs and ^{241}Am chronologies. It was important to determine whether these turbidite events correspond to instrumental and historical earthquakes generated in the eastern Taiwan margin.

To determine the Holocene timescale, the absolute chronology is usually based on ^{14}C measurements of carbonaceous samples, allowing accurate paleoenvironmental interpretations. ^{14}C ages of marine species must be corrected for differences between the ^{14}C age of surface water and the contemporaneous atmosphere prior to calculation of a calendar age. This is because the waters of the ocean are out of equilibrium with respect to the atmosphere, causing marine carbon-containing material to appear older than material formed at the same time on land (in equilibrium with the atmosphere). The difference in ^{14}C age of the global surface ocean compared to the atmosphere ^{14}C is termed the global marine reservoir age $R(t)$ (Stuiver and Polach 1977). The preindustrial global reservoir age is estimated at $R(t) = 405 \pm 22$ ^{14}C yr and a time-dependent correction is available by using the Marine04 calibration curve (Hughen et al. 2004). Several studies have suggested the possibility of significant deviations in regional marine reservoir signature from this average value (Goodfriend and Flessa 1997; Ingram and Southon 1997; Siani et al. 2001; Reimer and McCormac 2002; Southon et al. 2002; Fontugne et al. 2004). The second aim of this paper will be to estimate the modern reservoir ^{14}C age by comparing AMS ^{14}C ages with ages derived from corrected ^{210}Pb profiles and historical accounts of identifiable seismic events.

SETTING AND ANALYTICAL METHODS

To study the recent sedimentary record, we collected a box-core sample during the OR1-1013 survey (Figure 1). Box-core KS06B (37 cm long) was collected in 1947 m of water depth in a small-perched basin on the slope of Luzon Arc, north of Green Island off Taiwan (Lehu et al. 2015). Multidisciplinary analyses were performed, with particular attention given to grain-size variation and turbidite/hemipelagite differentiation. The sediment core was sampled at 1-cm intervals for grain-size analyses using a Coulter laser microgranulometer LS13 320 (size range from 0.4 μm to 2 mm). Chemical composition and X-ray images were acquired using an ITRAX core scanner at 2-mm intervals.

^{14}C dating was performed on 10 mg of handpicked planktonic foraminifera (*Globigerinae* species). ^{14}C analyses were conducted at the Laboratoire de Mesure ^{14}C (LMC14) on the ARTEMIS accelerator mass spectrometer in the CEA Institute at Saclay (Atomic Energy Commission). These ^{14}C analyses were done with the standard procedures described by Tisnérat-Laborde et al. (2001).

Dating of sedimentary layers was carried out using ^{210}Pb , ^{137}Cs , and ^{241}Am methods on a centennial timescale. These nuclides together with U, Th, and ^{226}Ra were determined by gamma spectrometry at the Géosciences Montpellier Laboratory. The 1-cm-thick sediment layers were finely crushed after drying, and transferred into small gas-tight polyethylene terephthalate (PETP) tubes (internal height and diameter of 38 and 14 mm, respectively), and stored for more than 3 weeks to ensure equilibrium between ^{226}Ra and ^{222}Rn . The activities of the nuclides of interest were determined using a Canberra Ge well detector and compared with the known activities of an in-house standard. Activities of ^{210}Pb were determined by integrating the area of the 46.5-keV photopeak. ^{226}Ra activities were determined from the average of values

derived from the 186.2-keV peak of ^{226}Ra and the peaks of its progeny in secular equilibrium with ^{214}Pb (295 and 352 keV) and ^{214}Bi (609 keV). In each sample, the ^{210}Pb excess activities ($^{210}\text{Pb}_{\text{ex}}$) were calculated by subtracting the (^{226}Ra supported) activity from the total (^{210}Pb) activity.

RESULTS AND DISCUSSION

Turbidite Layer Identification

As discussed in the previous section, core KS06B is located in an intraslope basin north of the Lutao volcanic island (Figure 1). The whole core is composed of alternating hemipelagic sediment and fine-grained turbidite facies. The hemipelagite facies (HP hereafter) are characterized by homogeneous clay with a low lithic fragment content (<20%). In core KS06B, these facies are usually represented by a grain size that is typically <10 μm (Figure 2).

Turbidite facies are recognizable by their coarser grain size and characteristic fining upward structure (Figure 2), as defined by the Bouma (1962) sequence. The coarser grain size usually indicates an “energetic” event in the sequence, relative to the background sedimentation (i.e. hemipelagite facies). Turbidite facies are also characterized by geochemical anomalies relative to the background signal. Figure 2 shows Fe and Ca content, which are representative of both terrestrial and biogenic calcareous environments.

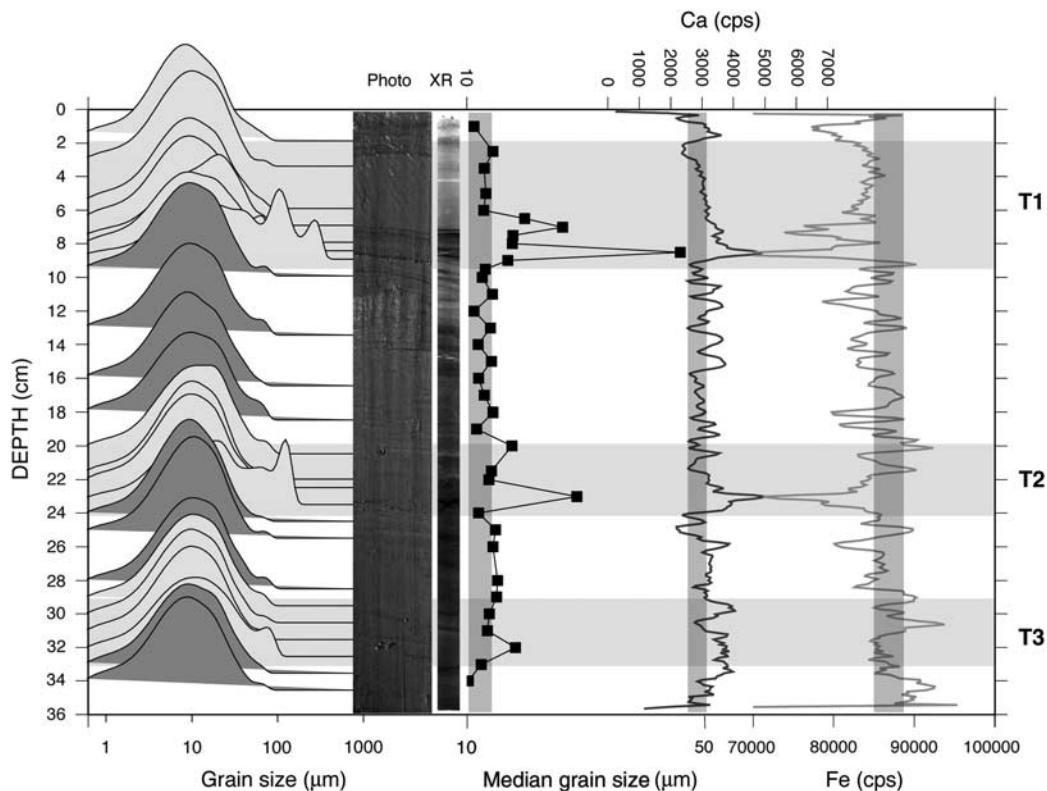


Figure 2 Sedimentological analysis of KS06-B and inferred turbidite events, based on grain-size distribution, photos, X-rays, median grain size, and chemical composition (Ca and Fe). Light horizontal bars highlight turbidite layers and light gray bars highlight the background signal of hemipelagic sedimentation.

In KS06B, we identified three events, hereafter referred to as T1, T2, and T3 (from top to bottom). Event T1 corresponds to a fine-grained turbidite composed of an 8.5-cm-thick silty-clay sediment on the top of a coarser silty basal layer (median grain size $\sim 35 \mu\text{m}$). Geochemical proxies show positive Ca anomalies that are anticorrelated with Fe anomalies (Figure 2). Analysis of the coarser sand fraction revealed a high biogenic content mainly composed of planktonic foraminifera, sponge spicules, and benthic foraminifera (Lehu et al. 2015). T2 is also interpreted as a fine-grained turbidite and is composed of a 4-cm-thick silty-clay sediment layer with a fine-silty basal layer (grain size $\sim 20 \mu\text{m}$). Their geochemical composition includes positive Ca anomalies that are anticorrelated with Fe anomalies. The sand fraction composition is characterized by a high proportion of biogenic material that reaches nearly 80% (Lehu et al. 2015). T3 is also regarded as a fine-grained turbidite. It is composed of a 5-cm-thick fining upward silty-clay sequence (grain size $\sim 15 \mu\text{m}$) with a sharp basal contact (Figure 2). Geochemical analysis reveals a very slight positive Ca anomaly that anticorrelates with a Fe anomaly (Figure 2). The coarser fraction of T3 has a higher biogenic content than observed for T1 and T2.

Radiochemical Measurements and ^{210}Pb Age-Depth Model

$^{210}\text{Pb}_{\text{ex}}$, ^{137}Cs , and ^{241}Am activity profiles of core KS06B are shown in Figure 3. The maximum $^{210}\text{Pb}_{\text{ex}}$ activity is observed at the top of the core (51.9 dpm/g) and decreases down to 35 cm depth (3.3 dpm/g). The ^{210}Pb activity versus depth curve is nonlinear (Figure 3A) and thus cannot be explained by radioactive decay alone. The activity within turbidite layers is particularly low as compared with hemipelagic layers and seems to be linked to grain-size variations and sediment deposits that have been reworked (Arnaud et al. 2002; Huh et al. 2004, 2006; Garcia-Orellana et al. 2006). This pattern is particularly evident in the sequences located between 2–9, 20–24, and 28–33 cm depth (Figure 3A). ^{137}Cs and ^{241}Am activity profiles present sharp peaks (5.8 and 3.6 mBq/g, respectively) at 19.5 cm and are near zero below 23 cm (Figure 3A).

In order to understand and establish an age-depth relationship in the KS06B core, we used the approach adopted by Arnaud et al. (2002) and assumed that hemipelagic sediments have been deposited with a constant accumulation rate and that turbidite layers represent instantaneous events. A synthetic sedimentary record is then built composed only of hemipelagic levels by removing the three turbidite events (T1, T2, and T3) from the sedimentary record (Figure 3B). This corrected $^{210}\text{Pb}_{\text{ex}}$ profile follows a nearly exponential curve (determination coefficient of 0.97) with the slope of the activity versus depth curve equal to 0.18 cm^{-1} . In this case, we can apply the CFCS model (Goldberg 1963; Krishnaswamy et al. 1971), which calculates an accumulation rate (AR) of $1.8 \pm 0.2 \text{ mm yr}^{-1}$ for all of the hemipelagic levels (Figure 3B). In order to determine the age of event T1 (2–9 cm), an AR of $1.8 \pm 0.2 \text{ mm yr}^{-1}$ was used for the corrected depth of 2–3 cm (without T1). Therefore, the T1 event would have occurred in $\text{AD } 2001 \pm 3$. Using the same approach, event T2 (20–24 cm) corresponds to $\text{AD } 1950 \pm 5$ and event T3 (28–33 cm) corresponds to $\text{AD } 1928 \pm 10$, near the limit of the ^{210}Pb method.

The most common dating method based on ^{137}Cs and ^{241}Am data (Robbins and Edgington 1975) assumes that the depth of maximum ^{137}Cs and ^{241}Am activities in the sediment corresponds to the maximum atmospheric production by nuclear bomb testing in 1962–1964. Cs can be highly mobile in marine sediments, following a preferential downward diffusive transport in porewater (Radakovitch et al. 1999). Despite the potential Cs mobility by diffusive transport, leading to the spreading of the Cs peak, we can see in Figure 3 that the ^{137}Cs profile shows a clear maximum (21 cm, which is equivalent to 10 cm in the corrected profile) corresponding to 1963. The ^{137}Cs and ^{241}Am activity depth profiles are highly consistent and both give an

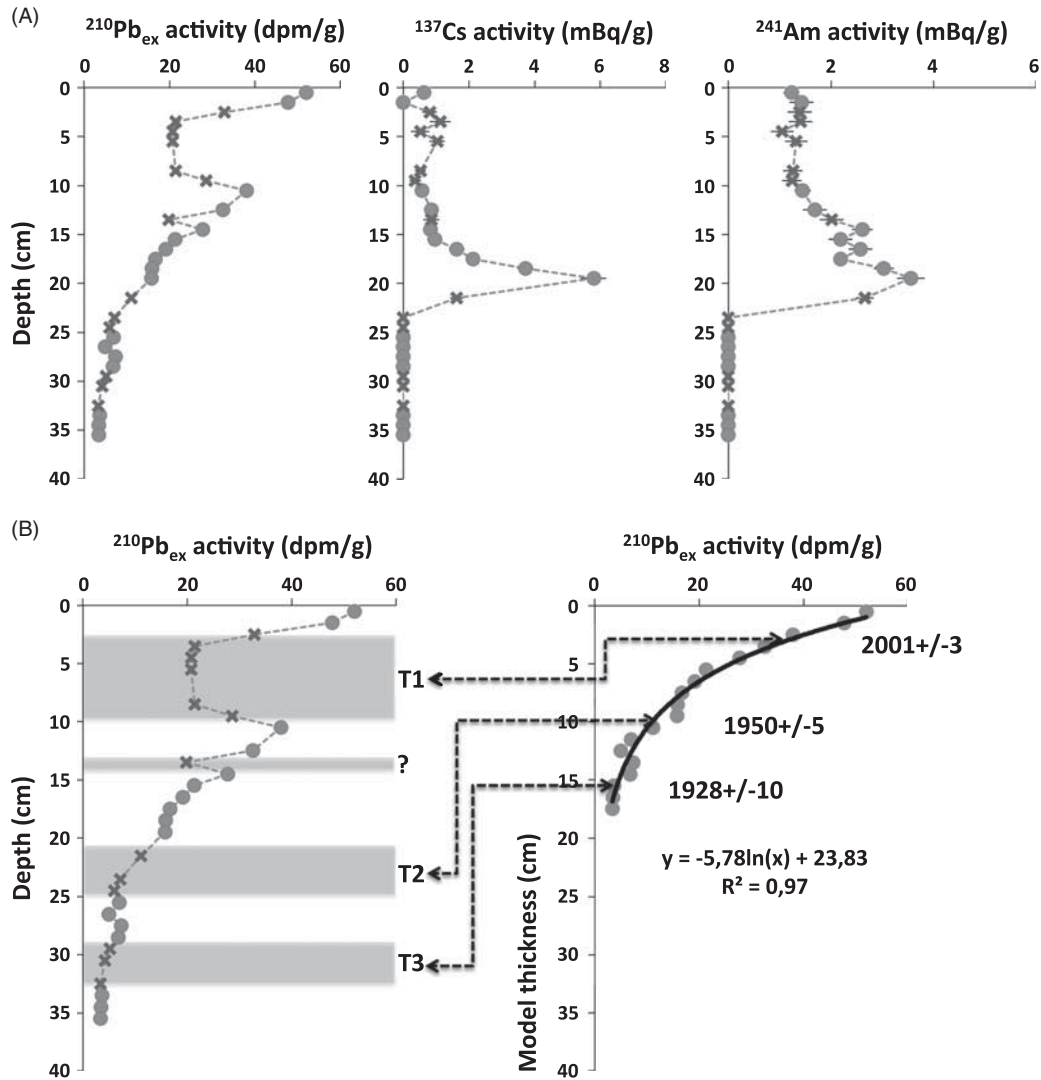


Figure 3 (A) ^{210}Pb , ^{137}Cs , and ^{241}Am activity profiles. Dots represent samples from continuous sedimentation (hemipelagite) whereas crosses represent samples from instantaneous sedimentation (i.e. turbidite events). (B) Graphical representation of the methodology used to reconstruct a depositional model to estimate sedimentation rate and turbidite layer ages.

accumulation rate of 1.84 mm yr^{-1} . This accumulation rate is in good agreement with ^{210}Pb ($1.8 \pm 0.2 \text{ mm yr}^{-1}$) and confirms our age-depth relationship.

Linking Turbidites to Earthquake Events

At site KS06B (Figures 1 and 4), earthquakes are the most likely explanation for triggering turbidity currents. The coring site is an isolated basin, without any sediment feeding from the continent. Hyperpycnal flows generated by typhoons cannot have an impact on this basin. Turbidite deposits likely are the result of local submarine instabilities of hemipelagic deposits generated by earthquakes. Moreover, in a previous offshore study from northeastern Taiwan, Huh et al. (2004) have shown that turbidites can be used as a paleoseismicity marker. As regards

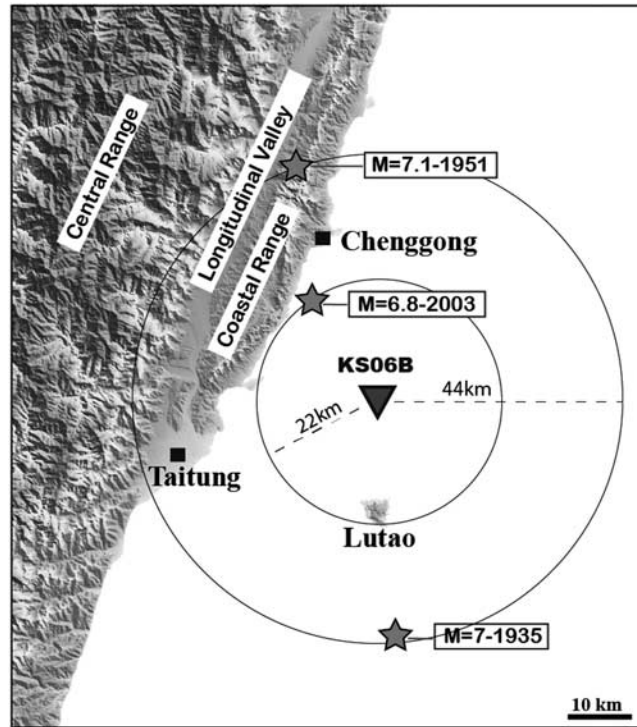


Figure 4 Distance from earthquake epicenters correlated with turbidite events to site KS06B.

the turbidite layers identified in core KS06B, the ^{210}Pb age of the near-surface event T1 corresponds to $\text{AD } 2001 \pm 3$. An examination of the catalog of large earthquakes in the eastern Taiwan margin shows a good temporal correlation with the 2003 Chengkong earthquake of M 6.8. The epicenter of this earthquake was located offshore, on the slope of the Coastal Range (Figure 4), about 22 km north of the location where core KS06B was collected. Although the effect of the earthquakes that occurred in the western foothills in 1999 (Chi-Chi earthquake, M 7.6) and in the southern Ryukyu subduction zone in 2002 (M 7) (see Figure 1 for locations) also occur within the time frame of T1, their epicenters were too far away to alter the sediment record preserved in the KS06B core. According to the empirical relationships established by Chung (2013), ground motion caused by an M 7 earthquake is insufficient to trigger slope failures at a distance greater than 50 km (Lehu et al., unpublished data). Indeed, the critical peak ground acceleration from which a slope usually starts to be destabilized is set as 0.1 g (Dan et al. 2009; Poudoux et al. 2014). Considering soft sediments conditions, these authors found that 0.1 g is reached at 50 km epicentral distance for an M 7 earthquake and at 100 km epicentral distance for an Mw 8 earthquake. The age of event T2 corresponds to $\text{AD } 1950 \pm 5$, which fits reasonably well with the 1951 Taitung earthquake of M 7.1. The epicenter of this earthquake was located on the emerged part of the Coastal Range, about 45 km north of the KS06B site. Finally, T3 corresponds to $\text{AD } 1928 \pm 10$ and can be correlated with a 1935 earthquake of M 7. The epicenter of that earthquake is located on the slope of the Luzon Arc south of Lutao Island, about 45 km from the coring site (Figure 4). It is worth noting that there is a remarkable correspondence between the only three $M \geq 6.8$ earthquakes that occurred within 50 km of the KS06B core and the three turbidites identified here.

MODERN RESERVOIR AGE ESTIMATION

Species living in ocean surface waters show older ^{14}C ages with respect to those living contemporaneously under atmospheric conditions. This difference, also known as the marine ^{14}C apparent age, is due to (1) oceanic circulation processes that tend to advect intermediate and deep ^{14}C -depleted water masses to the surface, (2) atmospheric ^{14}C changes, (3) air-sea CO_2 exchanges processes, and (4) hardwater effect due to the discharge of coastal rivers. Here, we present measurements of the reservoir ages of surficial waters in the Kuroshio Current (KC), which is still poorly known. Compared to the average modern ^{14}C marine reservoir age of $R(t) = 405 \pm 22$ ^{14}C yr, the KC ^{14}C reservoir age close to Taiwan displays a higher $R(t)$ value, with a deviance from the global mean sea surface reservoir age ΔR of 86 ± 40 ^{14}C yr (Yoneda et al. 2007; Yu et al. 2010). The ^{14}C depletion of the KC has been explained by the presence of water from the Pacific Equatorial Divergence with lower ^{14}C content (Yoneda et al. 2007; Yu et al. 2010).

Here, we estimate the modern sea surface reservoir ^{14}C age in KS06B by comparing ^{14}C values of planktonic foraminifera (*Globigerinae* species) with the ^{210}Pb chronology. As a reminder, KS06B was extracted in the eastern part of Taiwan and surface hydrographic conditions in that area are largely controlled by the KC. The first age on KS06B at 25 cm depth is 690 ± 30 ^{14}C yr. This age corresponds to a date of $\text{AD } 1950 \pm 5$, derived from the ^{210}Pb CFCS model (average sedimentation rate of 1.8 ± 0.2 mm/yr). The second age on KS06B at 33.5 cm depth is 695 ± 30 ^{14}C yr. This age corresponds to a date of $\text{AD } 1928 \pm 10$, also derived from the ^{210}Pb chronology.

Sea surface reservoir ^{14}C age $R(t)$ at 25 cm in KS06B was calculated by subtracting the atmospheric ^{14}C value estimated for the date of $\text{AD } 1950$ (199 ± 8 ^{14}C yr, Reimer et al. 2013) from the measured apparent ^{14}C ages of the depth at 25 cm (690 ± 30 ^{14}C yr, Table 1). This gives a $R(t)$ value of 491 ± 30 yr. The deviation from the global mean reservoir age (ΔR) is then obtained by subtracting the marine model age value estimated for $\text{AD } 1950$ (469 ± 23 ^{14}C yr, Reimer et al. 2013) from the measured apparent ^{14}C age at depth of 25 cm (690 ± 30 ^{14}C yr, Table 1). The ΔR value is thus estimated as 221 ± 38 yr (Table 1). By adopting a similar approach for a depth of 33.5 cm from core KS06B, dated to $\text{AD } 1928$ by the ^{210}Pb chronology (Table 1, Figure 5), we obtain $R(t) = 543 \pm 37$ ^{14}C yr ($\Delta R = 242$ yr ± 38 , Figure 5). These two dated depths suggest that in the study area, the average reservoir age $R(t)$ is 517 ± 48 ^{14}C yr and $\Delta R = 232 \pm 54$ yr.

This study gives a mean ΔR around 232 ± 54 ^{14}C yr ($n = 2$), which is substantially different from the previous estimation by using collections of pre-bomb shells, 86 ± 40 ^{14}C yr ($n = 9$; Yoneda et al. 2007; Yu et al. 2010). Our high ΔR value cannot be considered as a typical ΔR value for water belonging to the KC off Taiwan. On a local scale, different processes may increase ΔR values, such as hardwater effect or local upwelling. On a regional scale, a hardwater effect due to the discharge of coastal rivers was found to increase ^{14}C ages by 600 yr

Table 1 ^{14}C dates of modern pre-bomb foraminifera samples in KS06B and their reservoir ages.

Sample	^{210}Pb age (AD yr)	^{14}C age (BP)	Tree-ring ^{14}C age (BP) IntCal13	Reservoir age $R(t)$ (yr)	Model age Marine13	ΔR (yr)
KS06B-25	1950 ± 5	690 ± 30	199 ± 8	491 ± 31	469 ± 23	221 ± 38
KS06B-33.5	1928 ± 10	695 ± 30	152 ± 7	543 ± 37	453 ± 23	242 ± 38

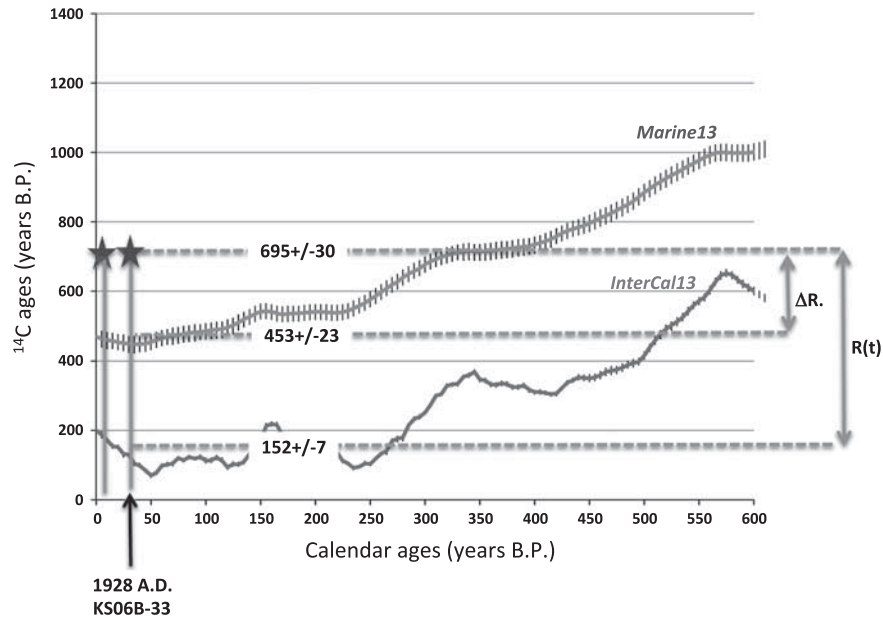


Figure 5 Sea surface reservoir ^{14}C ages $R(t)$ for modern samples on core KS06-B are calculated by subtracting the atmospheric ^{14}C age estimated by ^{210}Pb geochronology from the measured apparent ^{14}C ages of foraminifera. The deviance from the global mean reservoir age ΔR is obtained by subtracting the marine model value from the measured apparent ^{14}C age of the foraminifera.

in the Pierre Blanche lagoon in France (Sabatier et al. 2010). However, we consider that such a high ΔR value in our study area could not be due to the hardwater effect for the following reasons: (1) there are no limestone outcrops in the Taitung watershed, the most proximal watershed in the study area; and (2) a hardwater effect due to the discharge of coastal rivers is highly improbable because of the great distance of the KS06B from the nearest land of Taiwan (40 km away). In fact, the hardwater effect that affects terrestrial lakes, lagoons, and coastal areas has never been reported for the open marine environment, as mixing with seawater will quickly dilute any such effect—particularly here where the freshwater discharge from coastal rivers is deflected along the Taiwan coast by the strong Kuroshio Current.

Variations in regional oceanic activities, such as local upwelling, are most probably the cause of our high ΔR values. In our study area, an upwelling area in the KC has been identified north of Green Island off Taiwan. Vertical profiling with a shipboard lowered acoustic Doppler current profiler and a conductivity temperature depth profiler revealed sizable anomalies in flow and water characteristics in the lee of Green Island (Chang et al. 2013). The presence of Green Island induces upwelling and turbulence in the KC (Figure 6). In these zones, the water is colder and higher in chlorophyll-a concentration (Chang et al. 2013). These upwelling cells probably enhance the transport of relatively ^{14}C -depleted water to the surface, resulting in a more positive ΔR value in our zone.

In summary, the high ΔR value in our study area probably reflects active upwelling and not a hardwater effect. Moreover, as upwelling cells are local, our high ΔR value (232 ± 54 ^{14}C yr) must also be considered a local value. For water belonging to the KC off Taiwan, we consider the ΔR value of 86 ± 40 ^{14}C yr (Yoneda et al. 2007) to be more typical of the region.

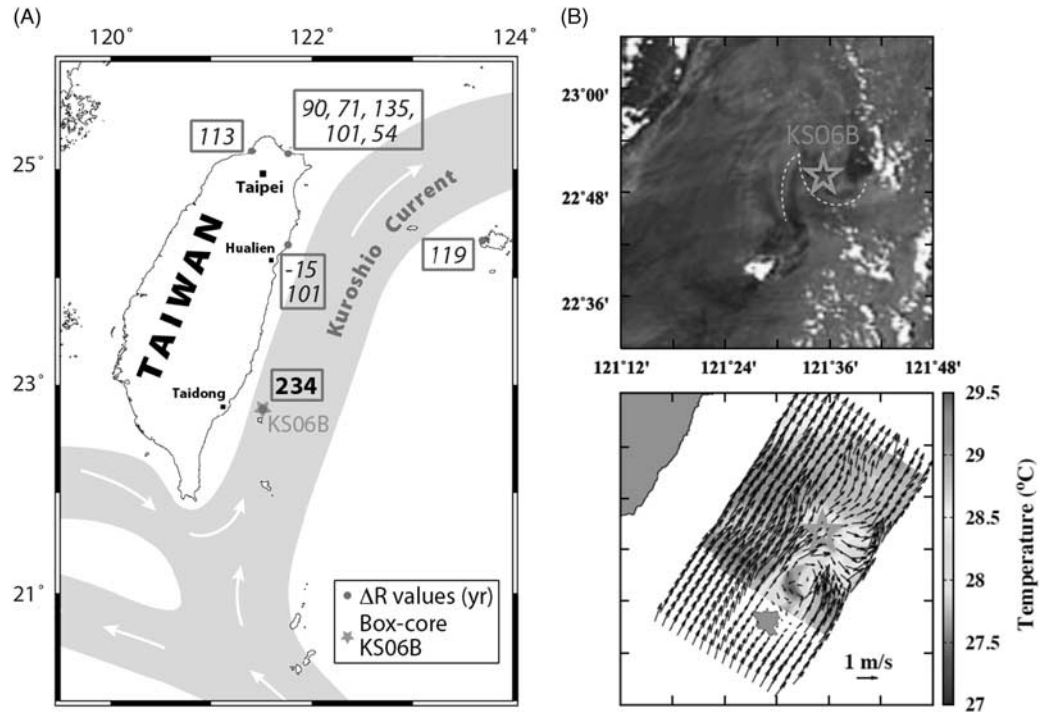


Figure 6 (A) General map of Taiwan showing the ΔR values around the Taiwan area (this study and Yoneda et al. 2007). In light gray: the mean path of the Kuroshio Current (after Hsin et al. 2008). The star shows the core location. (B) Upwelling zone north of Lutao Island evidenced by satellite image and seawater temperature (after Chang et al. 2013).

CONCLUSION

Based on $^{210}\text{Pb}_{\text{ex}}$, ^{137}Cs , and ^{241}Am activity profiles in a box core collected east of Taiwan, three turbidite events dated to $\text{AD } 2001 \pm 3$, $\text{AD } 1950 \pm 5$, and $\text{AD } 1928 \pm 10$ have been identified. These ages correspond to three $M \geq 6.8$ earthquakes that occurred in the region (< 50 km from the core site). These include (1) the 2003 Taitung earthquake (M 6.8), (2) the 1951 Chengkong earthquake (M 7.1), and (3) the 1935 Lutao earthquake (M 7.0). The good agreement between our estimated deposition time of the turbidites and the history of major local earthquakes suggests that the record of mass transport deposits can be used as a paleoseismic indicator in this high-convergence area (Lallemant et al. in press; Lehu et al. in revision).

The modern reservoir ^{14}C age (R) and the regional marine reservoir correction (ΔR) of the Kuroshio Current off Taiwan were estimated by comparing AMS ^{14}C ages with ages derived from a corrected ^{210}Pb profile. Our calculated mean ΔR value of 232 ± 54 ^{14}C yr ($n = 2$) is higher than the modern value of 86 ± 40 ^{14}C yr ($n = 9$, Yoneda et al. 2007). This high value is likely controlled by upwelling activities rather than by a hardwater effect. Local upwelling cells in the Kuroshio Current north of Green Island probably bring more ^{14}C -depleted water to the surface, resulting in a more positive ΔR value in that area.

ACKNOWLEDGMENTS

This project has benefited from the following financial support: National Central University (NCU) for ship time and analytical laboratory equipment, Institut National des Sciences de

l'Univers (INSU-CNRS) in the frame of "Aléas" program in 2013 and 2014 and Joint Research Projects between NSC and CNRS, LIA ADEPT Bureau de Représentation de Taipei (BRT) in France and France-Taiwan Foundation, and the French Institute in Taipei. We thank the Laboratoire de Mesure ^{14}C (LMC14) ARTEMIS in the CEA Institute at Saclay (French Atomic Energy Commission) for the ^{14}C analyses.

REFERENCES

- Arnaud F, Lignier V, Revel M, Desmet M, Beck C, Pourchet M, Charlet F, Trentesaux A, Tribouvillard N. 2002. Flood and earthquake disturbance of ^{210}Pb geochronology Lake Anterne, NW Alps. *Terra Nova* 14(4):225–32.
- Biq C. 1972. Dual-trench structure in the Taiwan-Luzon region. *Proceedings of the Geological Society of China* 15:65–75.
- Bouma AH. 1962. *Sedimentology of Some Flysch Deposits: A Graphic Approach to Facies Interpretation*. Amsterdam: Elsevier.
- Chang M-H, Tang TY, Ho C-R, Chao S-Y. 2013. Kuroshio-induced wake in the lee of Green Island off Taiwan. *Journal of Geophysical Research: Oceans* 118(3):1508–19.
- Chung J-K. 2013. Peak ground motion predictions with empirical site factors using Taiwan Strong Motion Network recordings. *Earth, Planets and Space* 65(9):957–72.
- Dan G, Sultan N, Savoye B, Deverchere J, Yelles K. 2009. Quantifying the role of sandy-silty sediments in generating slope failures during earthquakes: example from the Algerian margin. *International Journal of Earth Sciences* 98(4):769–89.
- Fontugne M, Carré M, Bentaleb I, Julien M, Lavallée D. 2004. Radiocarbon reservoir age variations in the South Peruvian upwelling during the Holocene. *Radiocarbon* 46(2):531–7.
- García-Orellana J, Gràcia E, Vizcaino A, Masqué P, Olid C, Martínez-Ruiz F, Piñero E, Sanchez-Cabeza J, Dañobeitia J. 2006. Identifying instrumental and historical earthquake records in the SW Iberian margin using ^{210}Pb turbidite chronology. *Geophysical Research Letters* 33: L24601.
- Golberg E. 1963. Geochronology with lead-210. In: *Radioactive Dating*. Vienna: International Atomic Energy Agency. p 121–31.
- Goodfriend GA, Flessa KW. 1997. Radiocarbon reservoir ages in the Gulf of California: roles of upwelling and flow from the Colorado River. *Radiocarbon* 39(2):139–48.
- Hsin Y-C, Wu C-R, Shaw P-T. 2008. Spatial and temporal variations of the Kuroshio east of Taiwan, 1982–2005: a numerical study. *Journal of Geophysical Research: Oceans* 113:C04002.
- Hughen K, Baillie M, Bard E, Beck J, Bertrand C, Blackwell P, Buck C, Burr G, Cutler K, Damon P, Edwards R, Fairbanks R, Friedrich M, Guilderson T, Kromer B, McCormac G, Manning S, Bronk Ramsey C, Reimer P, Reimer R, Remmele S, Southon J, Stuiver M, Talamo S, Taylor F, van der Plicht J, Weyhenmeyer C. 2004. Marine04: marine radiocarbon age calibration, 0–26 cal kyr BP. *Radiocarbon* 46(3):1059–86.
- Huh C-A, Su C-C, Liang W-T, Ling C-Y. 2004. Linkages between turbidites in the southern Okinawa Trough and submarine earthquakes. *Geophysical Research Letters* 31:L12304.
- Huh CA, Su CC, Wang CH, Lee SY, Lin IT. 2006. Sedimentation in the Southern Okinawa Trough—rates, turbidites and a sediment budget. *Marine Geology* 23(1–4):129–39.
- Ingram BL, Southon JR. 1997. Reservoir ages in eastern Pacific coastal and estuarine waters. *Radiocarbon* 38(3):573–82.
- Krishnaswami S, Lal D, Martin JM, Meybeck M. 1971. Geochronology of lake sediments. *Earth and Planetary Science Letters* 11(1–5):407–14.
- Lallemant S, Lehu R, Rétif F, Hsu S-K, Babonneau N, Ratzov G, Bassetti MA, Dezileau L, Hsieh M-L, Dominguez S. (in press). A 3000 years-old sequence of extreme events revealed by marine and shore deposits east of Taiwan, Tectonophysics.
- Lehu R, Lallemant S, Hsu S-K, Babonneau N, Ratzov G, Lin AT, Dezileau L. 2015. Deep-sea sedimentation offshore eastern Taiwan: facies and processes characterization. *Marine Geology* 369:1–18.
- Lehu R, Lallemant S, Hsu S-K, Ratzov G, Babonneau N, Ratzov G, Lin A-T, Dezileau L. (in review). Reconstructing 2,700 years earthquakes history using deep-sea turbidites offshore eastern Taiwan, Tectonophysics.
- Nittrouer CA, Sternberg RW, Carpenter R, Bennett JT. 1970. The use of Pb-210 geochronology as a sedimentological tool: application to the Washington continental shelf. *Marine Geology* 31(3–4):297–316.
- Pouderoux H, Proust J-N, Lamarche G. 2014. Submarine paleoseismology of the northern Hikurangi subduction margin of New Zealand as deduced from turbidite record since 16 ka. *Quaternary Science Reviews* 84:116–31.
- Radakovitch O, Charmasson S, Arnaud M, Bouisset P. 1999. ^{210}Pb and caesium accumulation in the Rhône Delta sediments. *Estuarine Coastal Shelf Sciences* 48(1):77–92.
- Reimer PJ, McCormac FG. 2002. Marine radiocarbon reservoir corrections for the Mediterranean and Aegean Seas. *Radiocarbon* 44(1):159–66.

- Reimer PJ, Bard E, Bayliss A, Beck JW, Blackwell PG, Bronk Ramsey C, Buck CE, Cheng H, Edwards RL, Friedrich M, Grootes PM, Guilderson TP, Hafflidason H, Hajdas I, Hatté C, Heaton TJ, Hoffmann DL, Hogg AG, Hughen KA, Kaiser KF, Kromer B, Manning SW, Niu M, Reimer RW, Richards DA, Scott EM, Southon JR, Staff RA, Turney CSM, van der Plicht J. 2013. IntCal13 and Marine13 radiocarbon age calibration curves 0–50,000 years cal BP. *Radiocarbon* 55(4):1869–87.
- Robbins J, Edgington D. 1975. Determination of recent sedimentation rates in Lake Michigan using Pb-210 and Cs-137. *Geochimica Cosmochimica Acta* 39(3):285–304.
- Sabatier P, Dezileau L, Blanchemanche P, Siani G, Condomines M, Bentaleb I, Piquès G. 2010. Holocene variations of radiocarbon reservoir ages in a Mediterranean lagoonal system. *Radiocarbon* 52(1):91–102.
- Seno T, Stein S, Gripp AE. 1993. A model for the motion of the Philippine Sea plate consistent with nuvel-1 and geological data. *Journal of Geophysical Research: Solid Earth* 98(B10):17,941–8.
- Siani G, Paterne M, Michel E, Sulpizio R, Sbrana A, Arnold M, Haddad G. 2001. Mediterranean sea surface radiocarbon age changes since the last glacial maximum. *Science* 294(5548):1917–20.
- Southon J, Kashgarian M, Fontugne M, Metivier B, Yim WWS. 2002. Marine reservoir corrections for the Indian Ocean and Southeast Asia. *Radiocarbon* 44(1):167–80.
- Stuiver M, Polach HA. 1977. Discussion: reporting of ^{14}C data. *Radiocarbon* 19(3):355–63.
- Suppe J. 1984. Kinematics of arc-continent collision, flipping of subduction, and back-arc spreading near Taiwan. *Memoir of the Geological Society of China* 6:21–33.
- Theunissen T, Font Y, Lallemand S, Liang W-T. 2010. The largest instrumentally recorded earthquake in Taiwan: revised location and magnitude, and tectonic significance of the 1920 event. *Geophysical Journal International* 183(3):1119–33.
- Tisnérat-Laborde N, Poupeau JJ, Tannau JF, Paterne M. 2001. Development of a semi-automated system for routine preparation of carbonate samples. *Radiocarbon* 43(2A):299–304.
- Yoneda M, Uno H, Shibata Y, Suzuki R, Kumamoto Y, Yoshida K, Sasaki T, Suzuki A, Kawahata H. 2007. Radiocarbon marine reservoir ages in the western Pacific estimated by pre-bomb molluscan shells. *Nuclear Instruments and Methods in Physics Research B* 259(1):432–7.
- Yu K, Hua Q, Zhao J, Hodge E, Fink D, Barbetti M. 2010. Holocene marine ^{14}C reservoir age variability: evidence from ^{230}Th -dated corals in the South China Sea. *Paleoceanography* 25:PA3205.